2Cm/x-
P.

NASA TECHNICAL TRANSLATION NASA TT F-14,509

(NASA-TT-F-14509) HEAT TRANSFER INVESTIGATIONS OF AXISYMMETRIC BODIES AT HYPERSONIC SPEEDS BY MEANS OF INFRARED MEASUREMENT (NASA) Aug. 1972 29 p CSCL 20M G3/33

N72-32934

Unclas
41010

HEAT TRANSFER INVESTIGATIONS OF AXISYMMETRIC BODIES AT HYPERSONIC SPEEDS BY MEANS OF INFRARED MEASUREMENT

Translation of: "Wärmeübergangs-untersuchungen an rotationssymmetrischen Flugkörpermodellen bei Hyperschallanströmung mittels des Infrarot-Messverfahrens," Deutsche Forschungs- und Versuchsanstalt für Luft- und Raumfahrt, Porz (W. Germany)/ Inst. für Angewandte Gasdynamik (DLR-Mitt-71-19), October 7, 1971, 35 pages.

NATIONAL AERONAUTICS AND SPACE ADMINISTRATION
WASHINGTON, D. C. 20546 AUGUST 1972

29 P.

TABLE OF CONTENTS

ABSTRACT. A new method of rapid heat transfer determination over surfaces of simple hypersonic models at a Mach number of 7.0 was examined and compared with other similar methods. The heat transfer measurements were performed in a hypersonic wind tunnel.

Abbreviations

/6[*]

c_p	specific heat at constant pressure
α	heat transfer coefficient
q	heat transfer value
λ	thermal conductivity
γ	specific gravity
l, x	depth of heat penetration
s	distance of a surface element from the stagnation point
R	model radius
M	incident flow Mach number
Re_{∞}	Reynolds number referred to 1 m
t	Time
t_D	time of heat penetration
T_u	color change, phase change, and isothermal temperature
T_r	adiabatic wall temperature
T_a	initial temperature

[*]Numbers in the margin indicate pagination in the original foreign text.

opening angle
integration variable
thermal conductivity

1. Introduction /7

Space flight bodies are exposed to high thermal stresses during reentry. The determination of these thermal processes and the treatment of problems of reducing heat transfer have for a long time been among the major objectives of theoretical and experimental studies in the hypersonic region.

The theoretical calculations of heat transfers at the stagnation point for hypersonic flying objects are generally confirmed by measurements [1]. The stagnation point thermal stress is quite dependent on the magnitude of the nose curvature [2, 3]. With blunt aircraft noses the penetrating heat can be conducted away well, and also there can be a considerable reduction of heat transfer in the stagnation region.

Theoretical considerations on heat transfer in aerodynamic bodies downstream from the stagnation point are limited to simple plane and rotationally symmetric body shapes, as fairly reliable assumptions on the pressure distributions to be expected can be applied (Newton's theory, Blast wave analogy) [3, 4, 5]. With complex models, one is generally directed toward experimental determination of the local surface pressures.

Shock wave wind tunnels are well suited for heat transfer measurements on simple models, as the test setup, measuring apparatus, and model production are relatively easily accomplished. Because of the temperature constancy of the transducer supporting material through the extremely brief measurement periods, good measuring accuracy is achieved [1, 5, 6]. But to provide a complex flight model (wings, control surfaces, fueslage combination) with suitable measurement elements such as film thermometers, thermocouples, etc., distributed over its entire surface sets up new requirements for manufacturing and measuring technology

(1)

In continuously or intermittently operating wind tunnels, the heat transfer distribution is in large part determined by means of non-contact temperature measurement (phase and color change methods) [7,8,9,10]. These methods have no high accuracy, to be sure, but they provide a good survey of the thermal stress over the whole flight structure. /8

In this report, we discuss the suitablilty of another method of non-contact temperature measurement, which was published long ago [11]. This discussion is presented by means of heat transfer measurements on four rotationally symmetric models in the H-1 wind tunnel. Here we deal with determining the thermal stress of a flight structure model with air flowing past it by means of an infrared camera. The manner of operation of this measuring system is explained below.

2. Working principle of the wind tunnel and experimental conditions.

The hypersonic wind tunnel, H-1, of the DFVLR Institute for Applied Gas Dynamics, Porz-Wahn, works on the blow-down principle (Figure 1). It consists of an electrically heated through-flow heater in which the air can be heated up to 1,400 °K, a conical nozzle with exchangable nozzle throats for the Mach numbers M = 6, 7, 9, 11, and 15, a measuring section with a diameter of 16 cm and schlieren-free glass windows on both sides for observation of the flow process. The downstream diffusor with an adjustable conical central body serves to achieve the necessary pressure recovery. The vacuum sphere which is connected ensures the pressure drops necessary for high Mach numbers and, because of a great volume of 2,000 m^3 and a high pump suction rate, makes possible performance of prolonged tests or continuous operation

(1) Translator's note: illegible in foreign text.

at high Mach numbers.

The measuring section is equipped with a charging mechanism which introduces the model into the measuring stream within 0.1 - 0.2 seconds. The time for passing through the measuring stream boundary zone, which is important for non-steady heat transfer measurements, thus, amounts to 0.01 - 0.02 seconds [21].

These investigations were done under the following flow conditions: /9

Incident Mach number	$M_\infty = 7.0$
Ambient pressure	$P_o = 5$ atmospheres abs.
Ambient temperature	$T_o = 673°K$
Reynolds number (1 = 1 m)	$Re_{\infty_N} = 1.643 \cdot 10^6$

For the tests of suitability of the measuring method introdced, models were selected for which both theoretical calculations and experimental results were available for the thermal stress occurring at hypersonic flow. The model series included a sphere with a diameter of 35 mm, the AGARD calibration model HB-1 with a 20 mm diameter, as well as two slender cones with different blunt nose shapes (Figure 2). The models are made of Teflon. Because of the low heat conductivity of this material, the tangential and normal thermal conduction of heat into the body wall are vanishingly small at appropriate test times. The material data for Teflon are taken from [12].

They are:

Thermal conductivity	$\lambda = 0.2 \frac{\text{kcal}}{\text{m} \cdot \text{hr} \cdot \text{degree}}$
Specific gravity	$\gamma = 2{,}200$ kg/m^3
Specific heat	$c_p = 0.25$ kcal/kg $\cdot$ degree

3. Measuring Procedure

In the following, the measuring procedures for non-contact temperature measurement used here are described, and their suitability for measurements in hypersonic wind tunnels of the design above is critically investigated.

3.1 Color change method /10

The use of colors which change with temperature for rapid approximate determination of heat transfer to model surfaces has already been described several times [7, 8, 15]. The model, made of a material with low heat conductivity, and with a thin coating of paint is placed into the flow as rapidly as possible and the time sequence of color changes is recorded by a photographic camera with medium to high picture rate. The magnitude of the heat transfer to a surface element then depends on the time between model insertion and color change at this point. The following error sources must be considered, however:

1) After the change, the coloring material often becomes grainy and forms bubbles, which can affect the flow around the model.

2. The color change is affected by the pressure at the model surface. At low pressures on the order of 1 Torr, deviations from the conversion temperature of up to 20% can appear [13].

3. The color change can be affected by moisture absorbed by the paint.

4. Photographic recording of the course of the color change requires good illumination of the model. Photo lamps of the usual design can falsify the measurement because of their high thermal radiation. Therefore, the use of daylight as the illuminant is recommended (e. g., cold light sources).

Because of the error sources mentioned, the entire method is calibrated. This calibration is preferably done by experimental studies with spheres, for which the local heat transfer curve is sufficiently well known.

3.2 Phase change methods /11

Recently, a method is often used for heat transfer determination which has significantly less error on the basis of accuracy and constancy of the color change than the use of the Thermocolor paints. Here we deal with a white paint (Tempilac) which, at a definite temperature, changes to a clear liquid [14, 15]. The only requirement is for a very thin paint coating so that no liquid particles migrate downstream and affect the flow.

3.3 Measuring methods with the infrared camera

Like the previously described methods, heat transfer determination using the infrared camera is also based on non-steady temperature measurement. But in contrast to the previously described methods, it is not the change of a color, but the infrared radiation from the model which is observed and recorded with a special camera. Figure 3 shows a photograph of the camera and its oscillograph. The optical system of the camera consists of an oscillating mirror and a rotating prism, which sample the model at a frequency of 16 Hz. An indium antimonide detector cooled with liquid nitrogen converts the incident infrared radiation into an electrical signal which can be made visible on the oscilloscope as a heat picture of the model being studied. Areas of different temperature appear on the image in gray tones of different brightness. Also, a definite temperature range (minimum of 0.1 °C) can be set on the oscilloscope for the determination of quantitative values. Lines or areas which correspond to this temperature then appear, analogous to the color change lines, on the picture with maximum intensity (white isotherms). The time course of the isotherms is also recorded here with a 16 mm photographic camera. The camera drive motor, running synchronously with the scanning mirror in the infrared camera, allows the recording of every other thermal image. Figure 4 shows the typical curve for an isotherm on a

spherical model with hypersonic incident flow. The white bar at /12
the lower edge of the picture indicates the temperature range which has been set. The picture sequence gives a good review of the various heat stresses occurring on a sphere. The relation between the actual model temperature and the infrared radiation registered depends essentially on the radiant emission of the model surface and the losses in the optical system of the camera. Determination of the model emission factor and calibration of the entire measuring method are, accordingly, absolutely necessary.

Figure 5 shows the experimental setup. In the background of the model there is a water-cooled plate. The model itself has a temperature which is higher by several degrees, so that with the inverse image setting it appears on the oscilloscope screen as a darker area. The infrared camera is directed perpendicular to the wind tunnel axis toward the model being studied, and is adjusted so that the model contour is sharply imaged on the screen.

Normal glass wind tunnel windows are not suitable for observation and recording of the radiation. The window is, accordingly, replaced by a thin plastic film which is supported against the low pressure in the measuring section by a perforated plate. This arrangement has proved good in previous measurements [11].

Let us mention briefly here some advantages of the method in comparison to other measuring methods:

1) simple model production
2) no falsification of the flow about the model by paint bubbles or liquid droplets
3) possibility of short-term tests, as the smallest temperature differences can be adjusted
4) the temperature range of the isotherms can be limited to a minimum of 0.1°C.

Disadvantages and error sources, as well as possibilities /13
for eliminating them, are indicated in the section on "measurements".

4. Measurements

4.1 Color change measurements (Thermocolor)

The measurements were made on a sphere. The change point for the paint used – the Thermocolor system of the Faber Castell company – was at 95°C, with a color change from rose to lilac. Under the given incident flow conditions, a color change as far as the model shoulder could be recorded within the maximum experimental duration determined by the thermal penetration time, which is determined approximately. The thermal penetration time is not affected by the heat transfer coefficient. It depends only on the thermal conductivity of the material as well as on the allowed thermal penetration depth. Within this time, the effect of thermal conduction in the model is considered to be negligibly small. A shortening of the experimental time, favorable for determination of heat transfer according to the single layer method, by use of colors with significantly lower change temperature ($\Delta T \approx$ 10°C - 20°C) could not be attained, as the change was severely falsified with dyes which react more sensitively, particularly by the effects of reduced pressure.

The results of the measurements are plotted in Figure 6 and Figure 7. Figure 6 shows the course of the color change as a function of the test period. It can be seen that the change occurs very rapidly at the stagnation point, so that the model insertion time must be extremely short for accurate measurements. The difficulty in determination of the heat transfer at the stagnation point is that the model surface is not evenly illuminated, so that the accuracy of the color change line is affected by shadow effects near the model outline, by as much as a spherical angle of φ = 25°. At the stagnation point itself the times characterizing the heat transfer can only be extrapolated by means
of the course of the curve. This yields large errors in determ- /14
ining this quantity. But because this quantity often serves as a reference value for the local heat transfer values on the entire

body, calculation according to known theories appears advisable [2, 3].

Because of the effects on the transition temperature mentioned in Section 3.1, the absolute magnitude of the heat transfer at a sphere cannot be determined directly from Figure 6. But, because of the well known heat transfer course, the sphere is often used as a calibration body for this method. For the running distances S/R plotted as a function of the running time, then, the heat transfer coefficients referred to the stagnation point value are determined according to Figure 8 from the theoretically determined heat transfer curve, and they are plotted as a function of the time in Figure 7. Local heat transfer conditions at the surfaces of arbitrary flight body configurations can be determined by means of this diagram, at the same incident flow conditions and with use of the same transition paints. Then the stagnation point value for the calibration sphere, α_0, must be recalculated for the corresponding nose radius of the model according to the Lees heat transfer formula.

For comparison, in Figure 8 the values obtained experimentally and by means of a computer method for a semi-infinite thick plate are plotted. The relation between the heat transfer coefficient and other characteristic parameters is determined here from the solution of the equation for unidimensional heat flow.

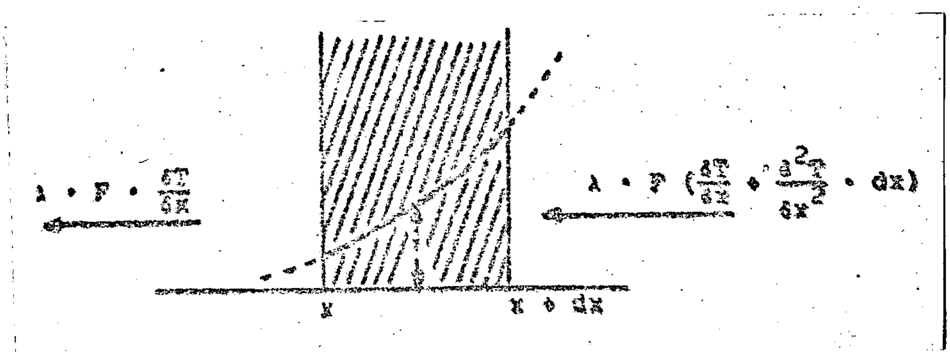

If one considers a surface element F of thickness dx, /15
then there appears at point x a heat flow which is smaller than that at point $x + dx$. The amount of the difference, $\lambda \cdot F \cdot (\delta^2 T/\delta x^2)\,dx$ is then equal to the amount of heat stored in the body element, if heat flows in the y-direction can be avoided.

$$c_p \cdot \gamma \cdot F \cdot dx \cdot \frac{\delta T}{\delta t} = \lambda \cdot F \cdot dx \cdot \frac{\delta^2 T}{\delta x^2} \cdot$$

The resulting differential equation for unidimensional heat flow is then:

$$\frac{\delta T}{\delta t} = \frac{\lambda}{\gamma \cdot c_p} \frac{\delta^2 T}{\delta x^2} \cdot$$

To solve this equation, the material coefficient is set constant. Furthermore, the following conditions must be fulfilled for an unambiguous evaluation:

1) The model has a homogeneous initial temperature before insertion.
2) The model is heated only at its surface during the experiment. The maximum heat penetration time in the experiment must not be exceeded.
3) The color change occurs at the corresponding surface temperature.

Under these conditions, the solution of the equation is:

$$\frac{Tu - Ta}{Tr - Ta} = 1 - e^{\beta^2} \cdot \mathrm{erfc}(\beta),$$

where

$$\beta = \frac{\alpha}{\lambda} \cdot \sqrt{\frac{\lambda}{\rho \cdot c_p} \cdot t}$$

$$\mathrm{erfc}(\beta) = \frac{2}{\sqrt{\pi}} \int_\beta^\infty e^{-\eta^2}\, d\eta,$$

The values of the parameter β are plotted in Figure 9 as /16
functions of the transition temperature. For given material coefficient and known color change times, the heat transfer coefficient can be determined from this.

The local heat transfer values calculated by this evaluation method (Figure 8) show good agreement with the data obtained from other measuring methods in the range of the sphere shoulder, while large variations appear in the vicinity of the stagnation point. Use of spheres as calibration models is possible for the evaluation of thermocolor measurements.

Data from other authors are plotted for comparison in Figure 8 (Hickman and Giedt [20]). The measurements were made in a low-density wind tunnel at M = 6 with a glass model equipped with resistance elements and also with a nickel model with thermocouples. The measurements agree approximately with the heat transfer curve calculated for M = 6 according to L. Lees.

4.2 Phase change measurements (Tempilac)

Figure 8 also shows data determined for the sphere by this method and evaluated according to the thermal conduction equation for unidimensional heat flow. Up to a distance from the stagnation point of S/R = 0.9, they agree well with the theoretical curve. The deviations in the shoulder region can be traced back, on one hand, to the surface pressure which deviates somewhat from the pressure curve determined by Newton's theory [16, 17] and, on the other hand, to markedly increasing thermal conduction in the body wall. Local surface pressures were not determined in this series of experiments.

4.3 Infrared Measuring method (Thermovision)

Local heat transfers were determined with the infrared camera for the test bodies specified from two experiments each with differing isotherm settings. For the sphere (Figure 8) the values of both /17 experimental series agree well, while deviations appear for the blunt cones, Figure 10 and Figure 11. The reason must be sought in the fact that neither the emission coefficient of the model material nor the temperature of the isotherm can be determined exactly without a suitable calibration method. In the experiments, a calibration curve furnished by the manufacturer was used. From our previous experience it appears desirable to calibrate before each experimental series by means of a calibration apparatus manufactured by the same company. This device is now available and will be included in the test setup for future measurements.

In the transition region "spherical nose - slender cone" the heat transfer curves for the blunt cones deviate from the theoretical curve, and approach it only at the tail of the body. One reason for this is, again, to be sought in a pressure curve departing from the theoretical values [18, 19].

For the AGARD Model HB-1 (Figure 12) the heat transfer values agree well with other measurements at $M = 20$ up to the beginning of the cylindrical part. The following deviations are due to the Mach number effect and to the measurement uncertainties mentioned above. Figure 13 shows schlieren pictures of the test model used.

5. Summary

An infrared camera was used in the H-1 hypersonic wind tunnel for rapid determination of thermal stresses on hypersonic flight structures. The advantages of this method over the previously common measuring methods with color changes were indicated and demonstrated by measurements on simple rotationally symmetric models. For optimal utilization of this system and to improve the measuring accuracy, improvements in the calibration method and a decrease in the effects of errors are necessary. For comparison with theoretical results, an accurate determination of the pressure course on the model surface is necessary.

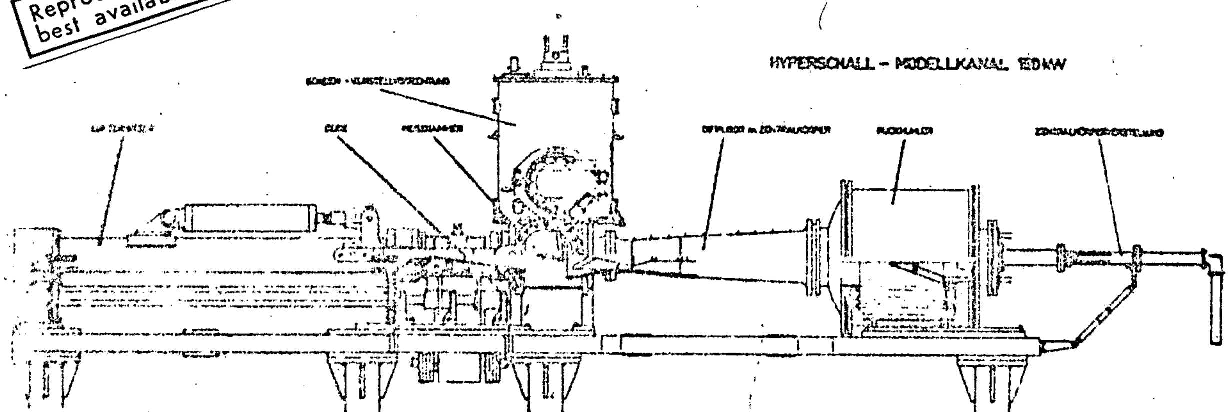

Figure 1. Wind tunnel plan

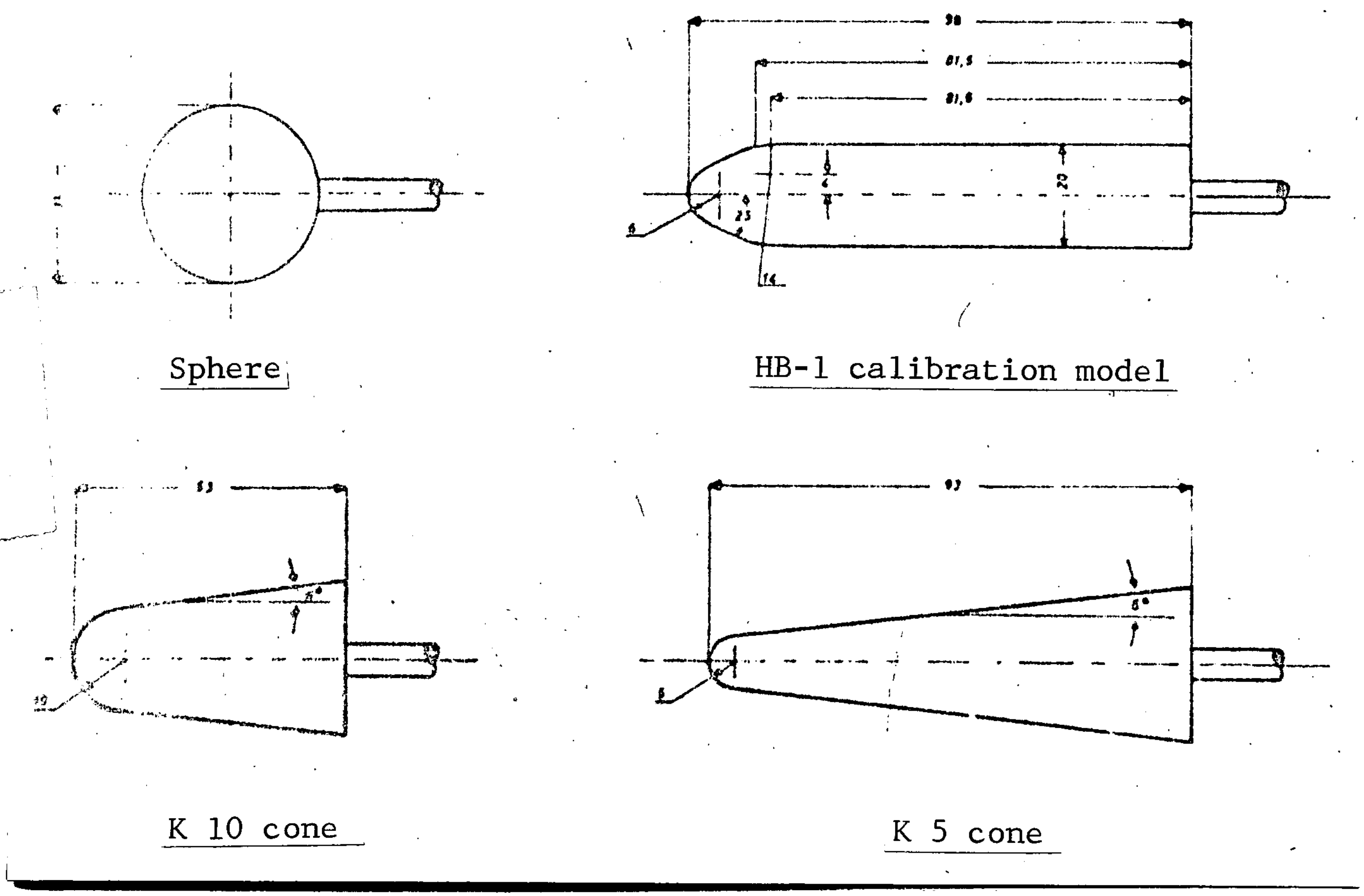

Figure 2. Model dimensions

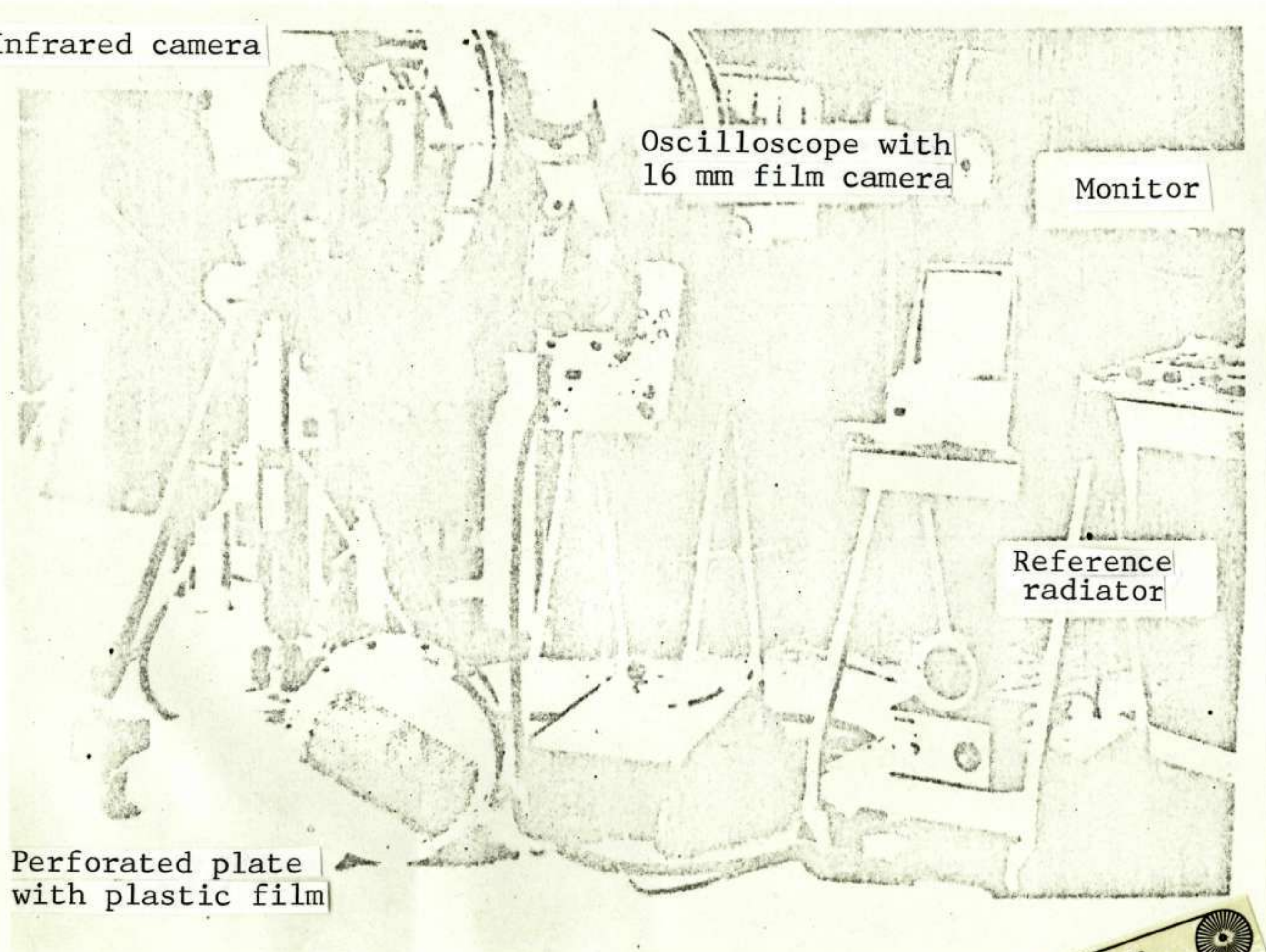

Figure 3. Infrared camera with its oscilloscope

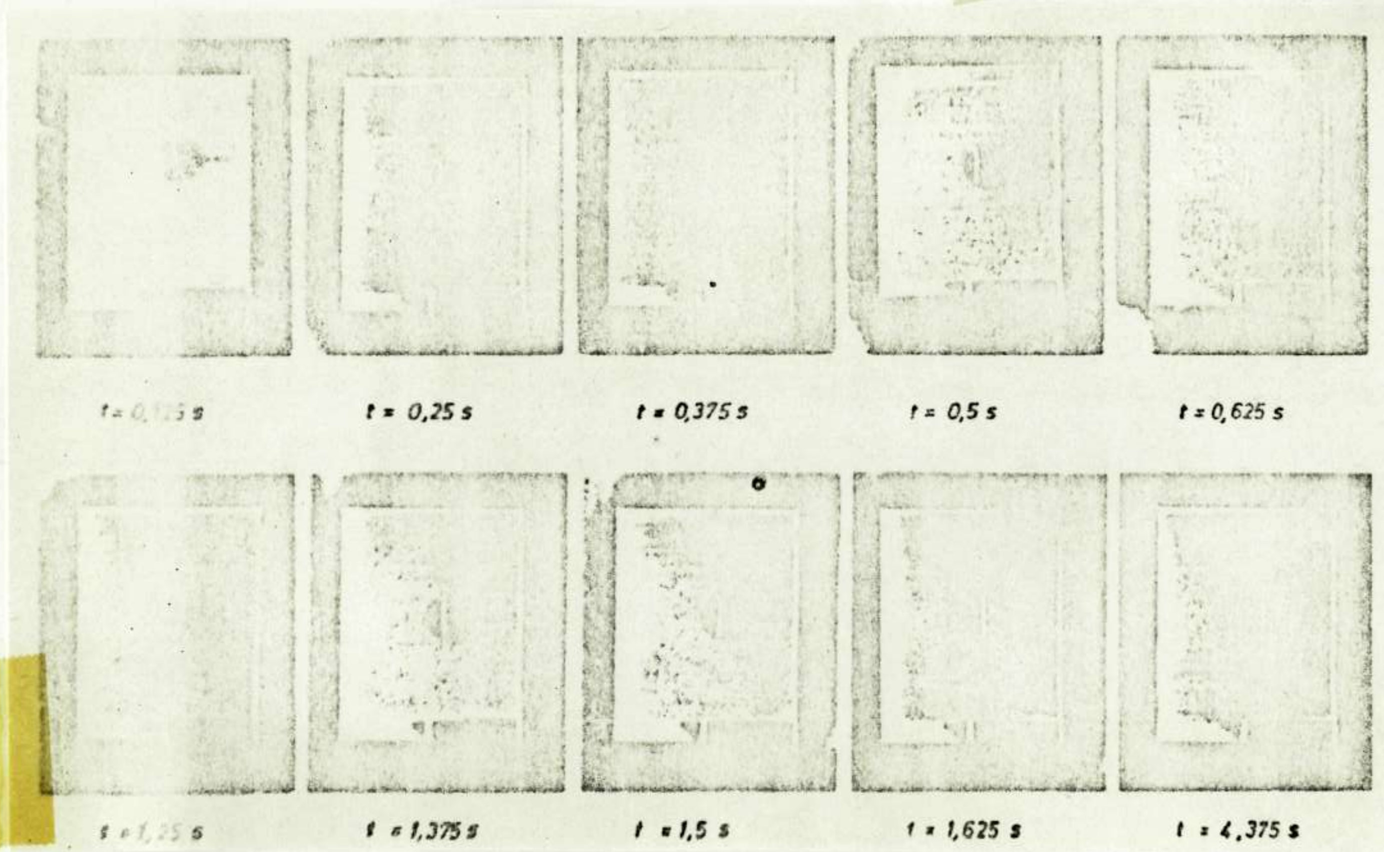

Figure 4. Course of the isotherm on a sphere

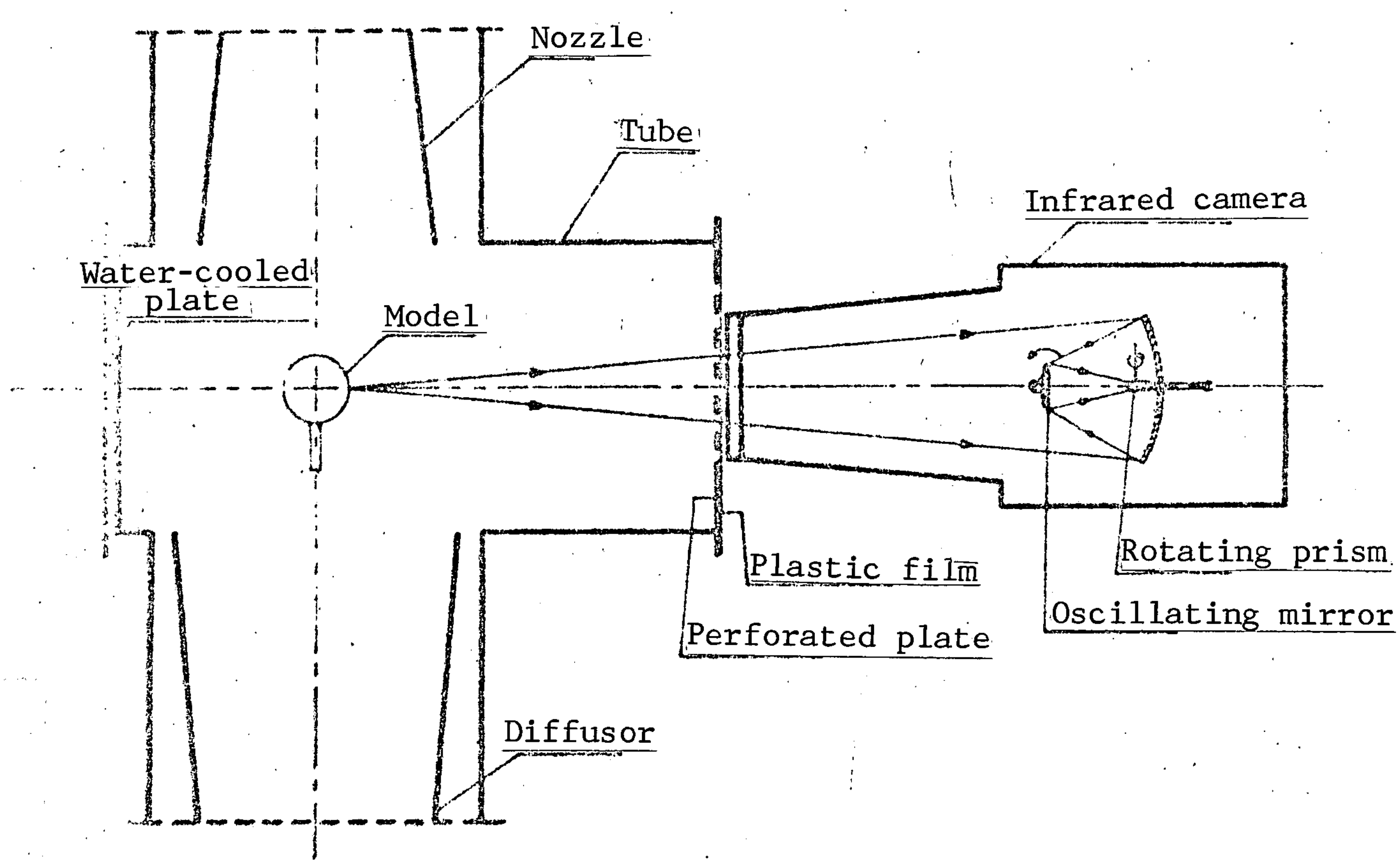

Figure 5: Design of the infrared measuring method

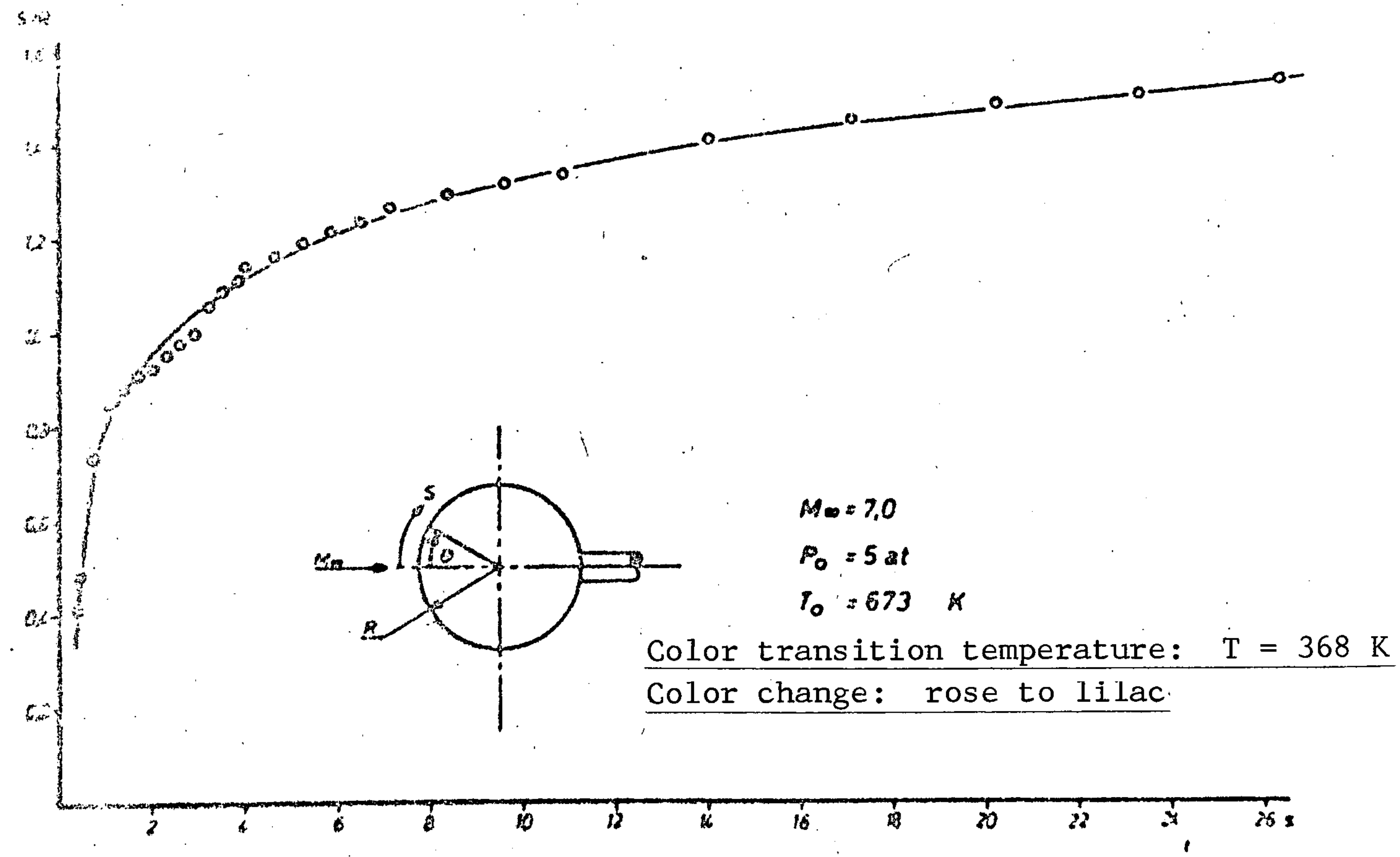

Figure 6. Color change on a sphere (R = 17.5 mm) as a function of the experimental time

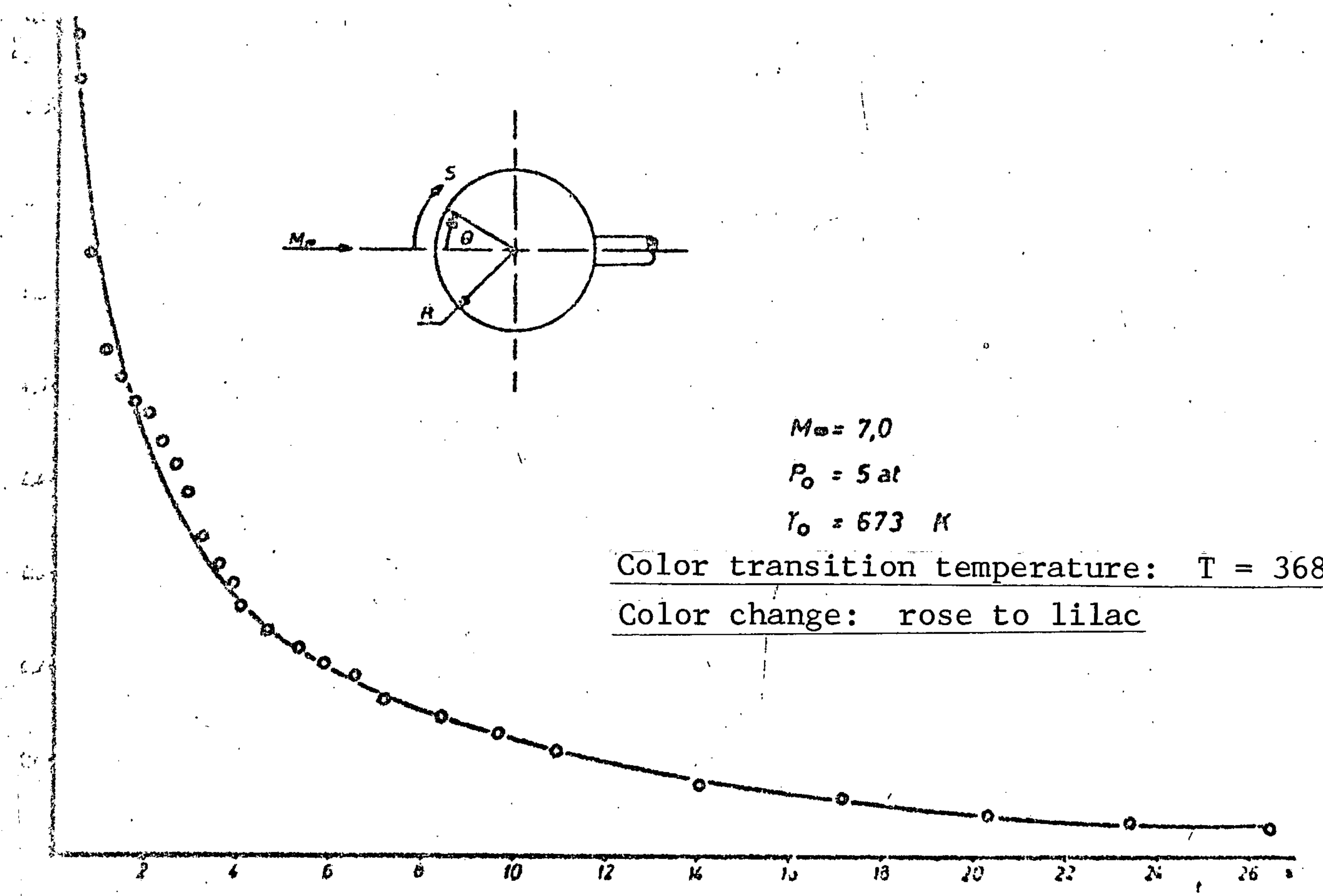

Figure 7. Ratio of the heat transfer coefficients for a sphere (R = 17.5 mm) as a function of the experimental time

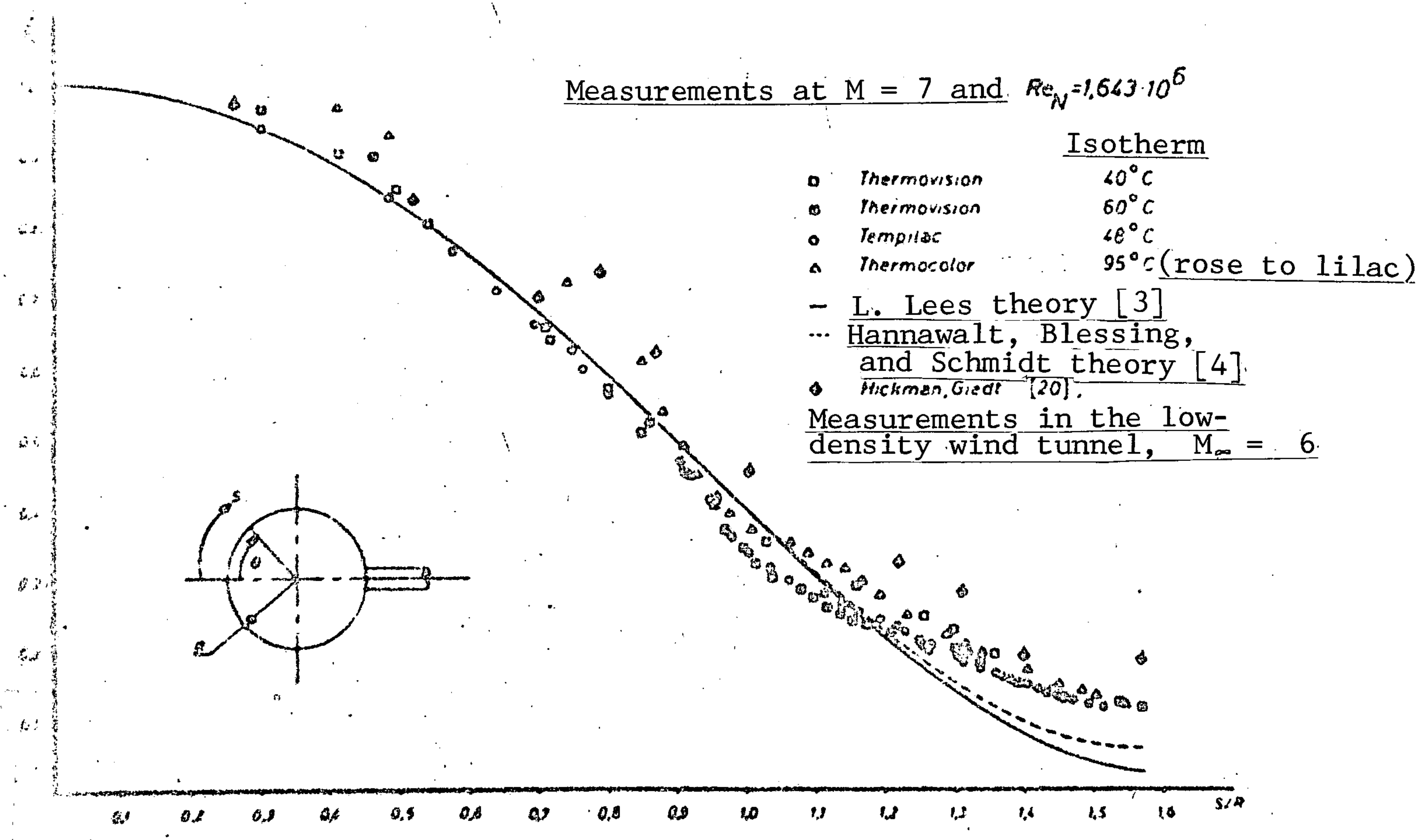

Figure 8. Local heat transfer on a sphere

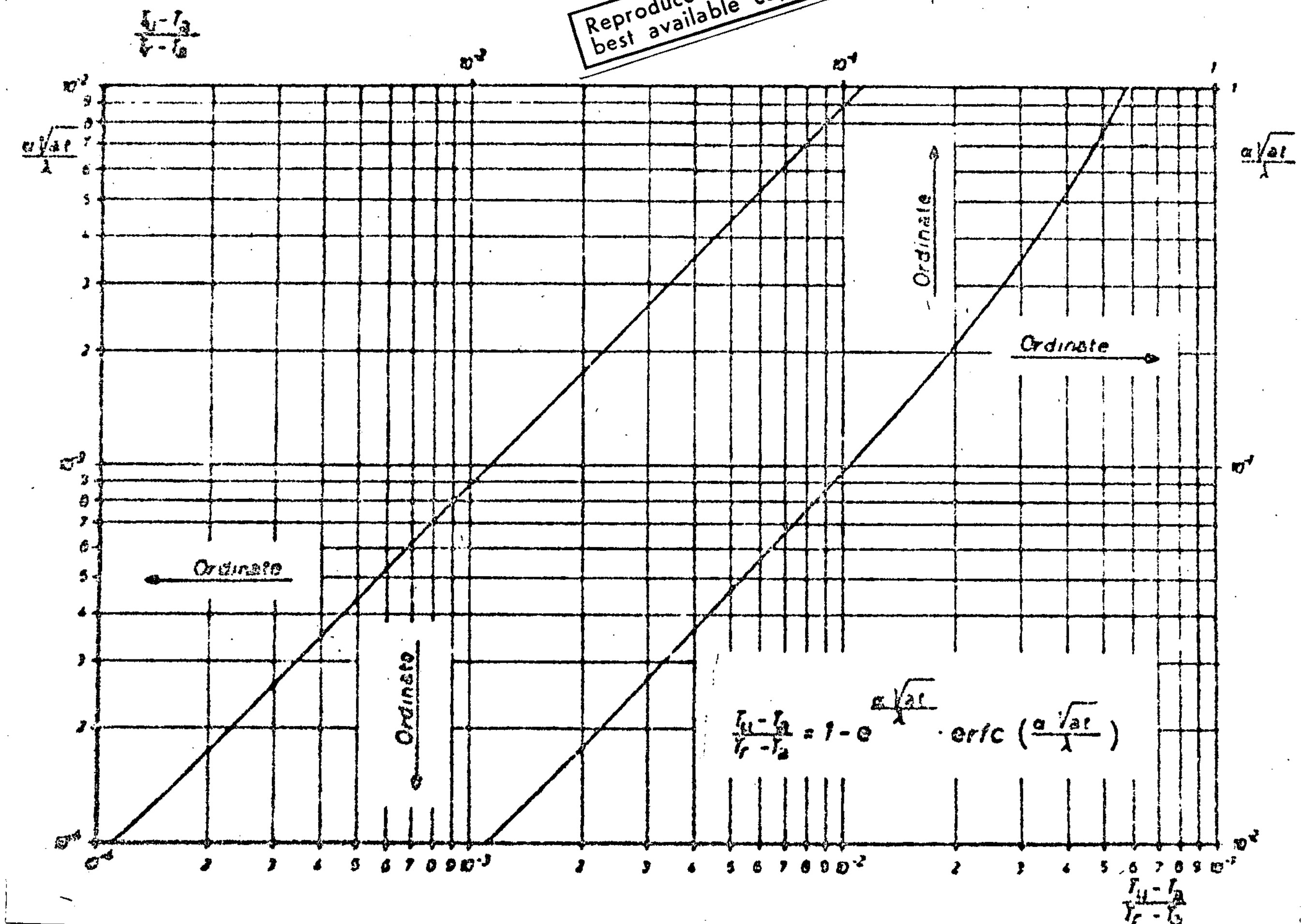

Figure 9: Solution of the heat transfer equation for semi-infinite thick plates

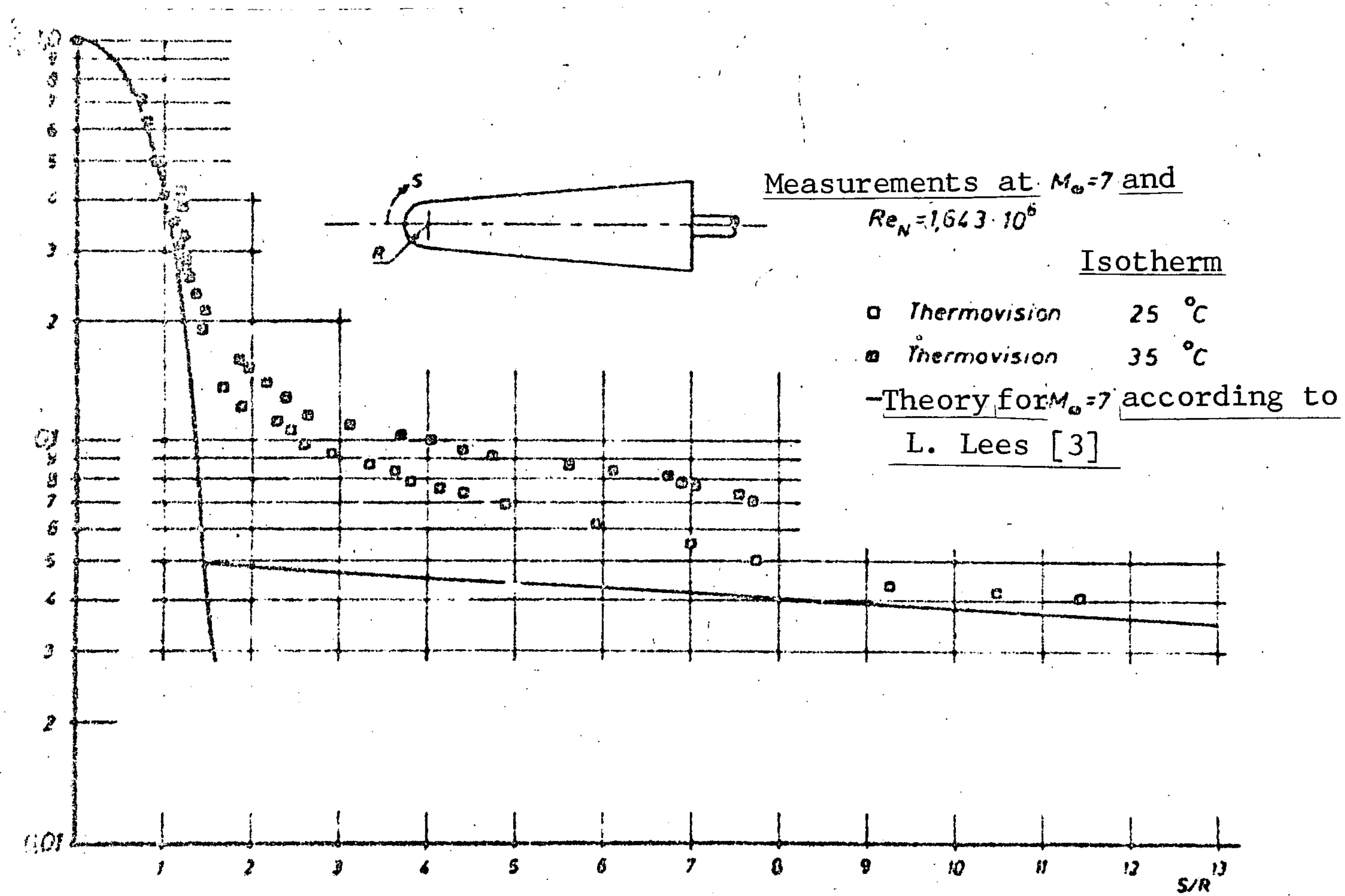

Figure 10. Local heat transfer on the K 5 cone

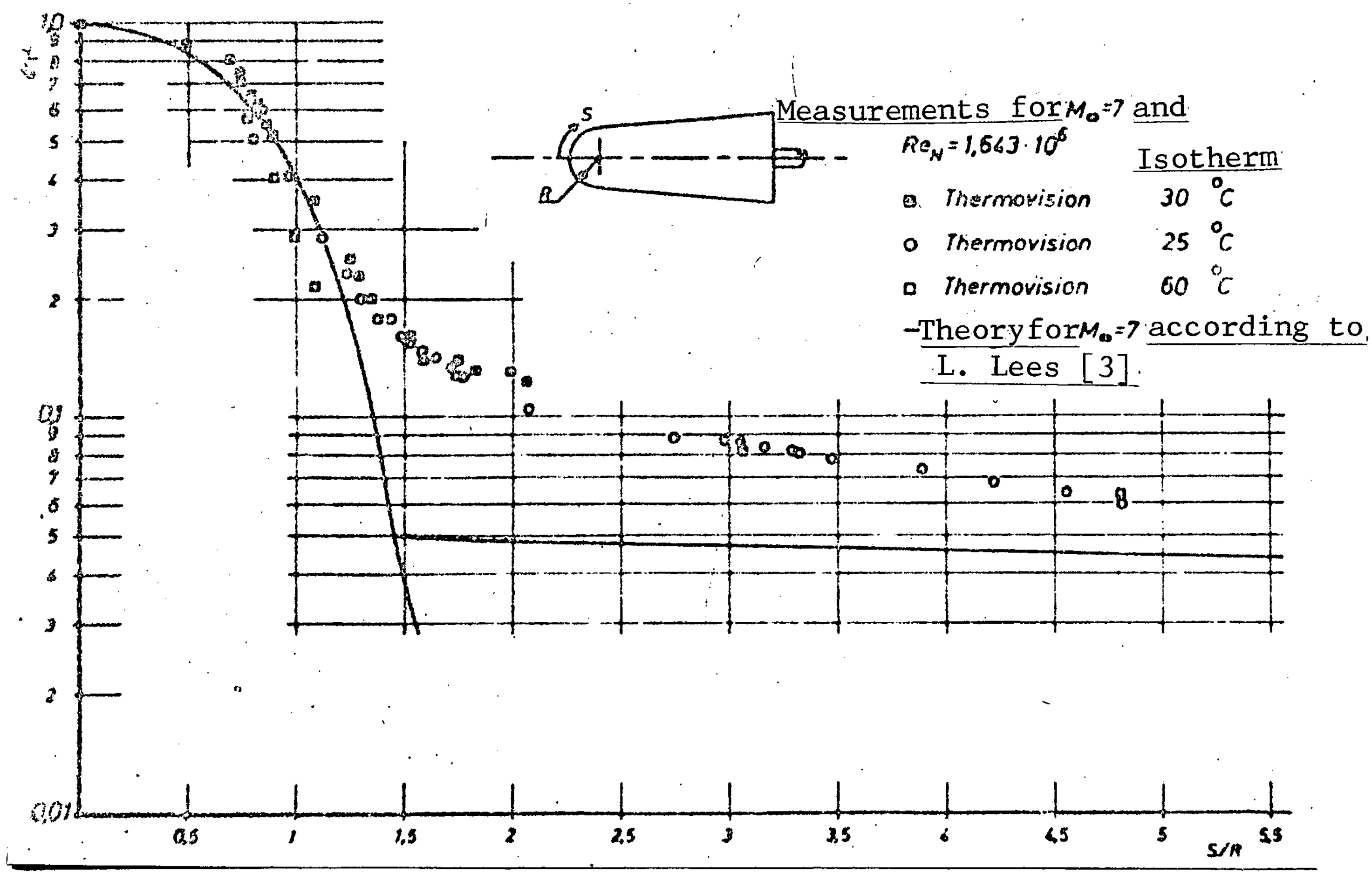

Figure 11: Local heat transfer on the K 10 cone

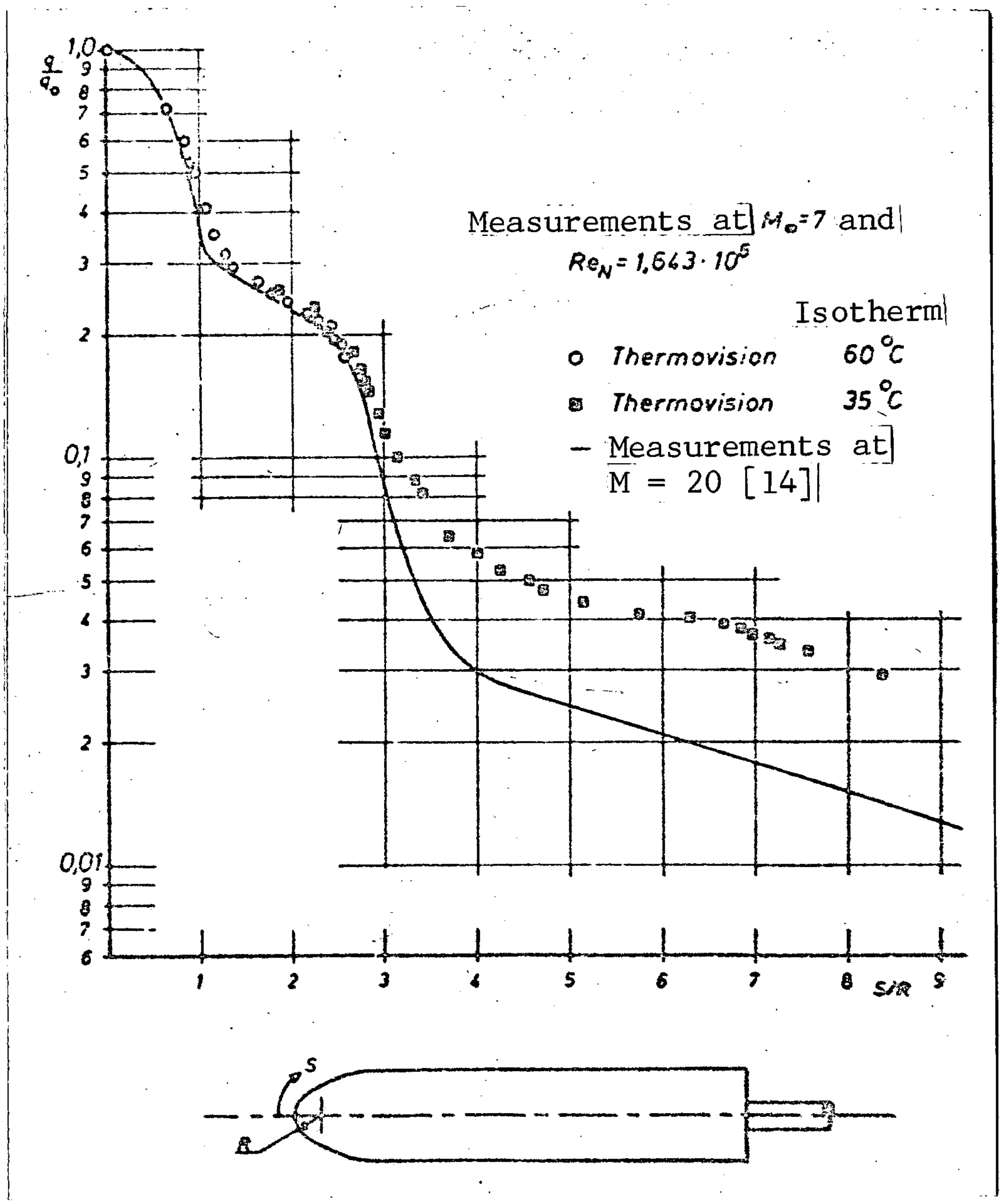

Figure 12. Local heat transfer on the AGARD HB-1 calibration model.

Spherical model ($R = 17,5\ mm$)

$M_\infty = 7,0$

$P_0 = 5\ at$

$T_0 = 673\ K$

Blunt cone ($K\,10$)

$M_\infty = 7,0$

$P_0 = 5\ at$

$T_0 = 673\ K$

Blunt cone ($K\,5$)

$M_\infty = 7,0$

$P_0 = 5\ at$

$T_0 = 673\ K$

AGARD HB-1 calibration model

$M_\infty = 7,0$

$P_0 = 5\ at$

$T_0 = 573\ K$

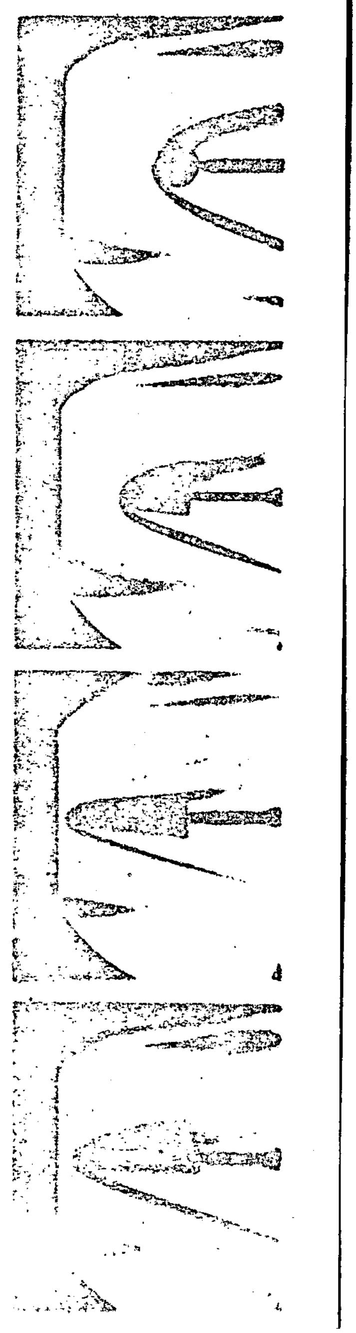

Figure 13. Schlieren photographs of the test models

REFERENCES /19

1. Rose, P.H. and W.I. Stark. Stagnation Point Heat Transfer Measurements in Dissociated Air. J. Aeron. Sci., Vol. 25, 1958, pp. 86 - 97.

2. Fay, J.A. Theory of Stagnation Point Heat Transfer in Dissociated Air. J. Aeron. Sci., Vol. 25, 1958, pp. 73 - 85.

3. Lees, L. Laminar Heat Transfer over Blunt-Nosed Bodies at Hypersonic Flight Speeds. Jet Propulsion, Vol. 26, 1956, pp. 259 - 269.

4. Hannawalt, A.J., A.H. Blessing and C.M. Schmidt. Thermal Analysis of Stagnation Regions with Emphasis on Heat Sustaining Nose Shapes at Hypersonic Speeds. J. Aero/Space Sci., Vol. 26, 1959, pp. 257 - 263.

5. Kemp, N.H., P.H. Rose and R.W. Detra. Laminar Heat Transfer Around Blunt Bodies in Dissociated Air. J. Aero/Space Sci., Vol. 26, 1959, pp. 421 - 430.

6. Wyborny, W., H.P. Kabelitz, H.J. Schepers. Resistance and Heat Transfer Measurements for Cylindrical Bodies with Hollow Spaces at Hypersonic Mach Numbers. WOLR-Jahrbuch, 1967, pp. 241 - 247.

/20

7. Sartell, R.J. and G.G. Lorenz. A New Technique for Measurement Aerodynamic Heating Distributions on Models of Hypersonic Vehicles. Proc. Heat Transfer and Fluid Mechanics Institute, Berkeley, Calif., 1964, pp. 130 - 146.

8. Kafka, P.G., J. Gaz, and W.T. Yee. Measurement of Aerodynamic Heating of Wind Tunnel Models by Means of Temperature Sensitive Paint. J. Spacecraft, Vol. 2, No. 3, 1965.

9. Jones, R.A. and J.L. Hunt. An Improved Technique for Obtaining Quantitative Aerodynamic Heat Transfer Data with Surface Coating Materials. J. Spacecraft, Vol. 2, No. 4, 1965.

10. Jones, R.A. and H.L. Hunt. Use of Fusible Temperature Indicators for Obtaining Quantitative Aerodynamic Heat Transfer Data. NASA TR-R-230, 1966.

11. Thomann, H. and B. Frisk. Measurement of Heat Transfer with an Infrared Camera. Int. J. Heat Mass Transfer, Vol. 11, 1968, pp. 819 - 826.

12. Diels, K. and R. Jaeckel. Leybold Vacuum Pocket Book. Springer Verlag, 1958.

13. Zimmler, A. Range of Applicability of Surface Temperature Determination by the Color Change Method. Reprint: Haus der Technik, Essen, Heft 218, pp. 12 - 20.

14. Gray, J.D. Summary Report on Aerodynamic Characteristics of Standard Models HB-1 and HB-2. AEDC TDR-64-137, July, 1964. /21

15. Ceresuela, R., A. Betremieux and J. Caders. Measurement of Kinetic Heating in a Hypersonic Wind Tunnel by Means of Thermosensitve Paint. La Recherche Aerospatiale, No. 109, 1965.

16. Vas, I.E., S.M. Bogdonoff and A.G. Hammitt. An Experimental Investigation of the Flow over Simple Two Dimensional and Symmetric Bodies at Hypersonic Speeds. WADC TN 57-146, 1957.

17. Julius, J.D. Experimental Pressure Distributions over Blunt Two- and Three-Dimensional Bodies Having Similar Cross Sections at a Mach Number of 4.95. NASA TN-D-157, 1959.

18. Oliver, R.E. An Experimental Investigation of Flow over Simple Blunt Bodies at a Nominal Mach Number of 5.8. Galcit Memo, No. 26, 1955.

19. Cleary, J.W. An Experimental and Theoretical Investigation of the Pressure Distribution and Flow Fields of Blunted Cones at Hypersonic Mach Numbers. NASA TN-D-2969, 1965.

20. Hickman, R.S. and W.H. Giedt. Heat Transfer to a Hemisphere-Cylinder at Low Reynolds Numbers. AIAA-Journal, Vol. 1, No. 3, March, 1963. /22

21. Pfeiffer, H., E. Will and H.D. Distelrath. The DVL H-1 Hypersonic Pilot Tunnel. DLR FB 69-44, 1969.